MASTER

CONF-780488--6

LA-UR-78-2276

TITLE:

FLUORESCENCE POLARIZATION AND PULSE WIDTH ANALYSIS OF CHROMOSOMES BY A FLOW SYSTEM

AUTHOR(S):

L. Scott Cram, Donna J. Arndt-Jovin, Brian G. Grimwade, and Thomas M. Jovin

SUBMITTED TO:

In: Proceedings of the Sixth Engineering Foundation Conference on Automated Cytology, Elmau, west Germany (April 23-29, 1978), Brian H. Mayall and Barton L. Gledhill, Eds. (Journal of Histochemistry and Cytochemistry)

los alamos
scientific laboratory
of the University of California
LOS ALAMOS, NEW MEXICO 87545

Form No. 836
St. No. 2629
1/75

UNITED STATES
ENERGY RESEARCH AND
DEVELOPMENT ADMINISTRATION
CONTRACT W-7405-ENG. 36

Running Title:

Polarization and Pulse Width Analysis of Chromosomes

I Copy for Larry

Q.

FLUORESCENCE POLARIZATION AND PULSE WIDTH ANALYSIS OF CHROMOSOMES BY A FLOW SYSTEM

L. SCOTT CRAM, DONNA J. ARNDT-JOVIN,
BRIAN G. GRIMWADE AND THOMAS M. JOVIN

Abteilung Molekulare Biologie, Max-Planck-Institut für Biophysikalische Chemie, D-3400 Göttingen, FRG

ABSTRACT

Isolated Chinese hamster chromosomes have been analyzed using a multiparameter computer-controlled cell sorter (MACCS) to obtain information about unique properties of individual chromosomes. Parameters other than DNA content were sought that would further aid in distinguishing among chromosomes. The polarized emission of Hoechst 33342 was measured for each class of chromosomes identified by a distinct peak. The emission anisotropy values for every chromosome class was a constant (E_A = 0.30) with chromosome size and DNA content. Pulse width was found to be a good parameter for resolving chromosomes, presumably according to arm length.

INTRODUCTION

Metaphase chromosomes are most often described by their arm length, area, DNA content, and banding patterns. Because it is important to be able to rapidly and accurately classify chromosomes into their different classes, the automated measurement of these parameters as well as others is being pursued from several directions (5,10,13). One technique is flow system measurement and flow sorting (8,12,23). DNA content has been the chromosome parameter measured in flow systems to date. Species such as Indian muntjac that have a low diploid number (2n = 7) can be completely characterized using this one parameter. A good correlation between the peaks in the DNA distribution and the chromosomes of the karyotype can be made (7). More complex karyotypes can not be uniquely described using the flow system on the basis of DNA content alone. For these cases, additional parameters measured in combination with DNA content have been investigated. We report here the first application of two analytical techniques for analyzing individual chromosomes in a flow system; the emission of polarized light from chromosomes stained with the dye Hoechst 33342 and pulse width analysis of the same chromosomes. These measurements were made using a multiparameter computer controlled cell sorter (MACCS).

When using the well polarized light of a laser for excitation, as is done in most flow cytometers, those chromophores with dipoles most favorably oriented with respect to the polarization of the laser beam will be preferentially excited. Likewise the

fluorescent emission will be polarized but is not usually analyzed. The molecular motion of the fluorescent molecule in its binding site during the lifetime of the fluorescent state will depolarize the emission. Emission anisotropy is a measure of the depolarization and therefore is a function of these parameters. Emission anisotropy (EA) is measured by quantitating the fluorescent intensities polarized parallel ($I_{||}$) and perpendicular ($I_{\perp}$) to the plane of polarized incident light. The EA is calculated from these measurements on a per cell basis using the relation: $EA = (I_{||} - I_{\perp})/(I_{||} + 2I_{\perp})$, (ref. 14). Any prefered orientation of the dye molecules in an isotropic system such as exists with oriented chromosomes will also affect the intensity of fluorescence in one plane of emission or the other. Basu (6) has recently measured the fluorescence polarization of aligned, acridine orange stained Chinese hamster chromosomes in a static system and reports a small but negative (-8%) polarization of fluorescence. This result indicates that when a fluorescent planer molecule is made to stack between the DNA base pairs, a non-random orientation of the base pairs within the chromosome can be detected. Orientation has not been of concern in previous work with polarized emission measurements in flow systems as only isotropic situations such as cells have been examined (3,11,18,20).

The measurement of chromosome arm length has been vigorously pursued for many years using sophisticated optical techniques (5) combined with complex normalization protocols (17). The importance of this parameter for resolving the human karyotype

is quickly realized from a two parameter plot of centromeric index (ratio of the large arm to total length) verses DNA content (19). Thus it would be extremely important, for the automated resolution of the human karyotype, to be able to simply avoid the problems of measuring chromosome curvature and detecting obscured chromatid tips. These problems can be avoided by aligning chromosomes in a flow stream and measuring the time duration of the fluorescent signal as the chromosome passes through a beam of exciting light. Consequently, we have undertaken a theoretical and experimental study of pulse shapes which can be expected for stained chromosomes in suspension traversing a focused Gaussian laser beam.

MATERIAL AND METHODS

Chromosome Preparation

Chromosomes were prepared from a clonal derivative (650A) of M3-1 male Chinese hamster cells kindly provided by Dr. A. V. Carrano, Lawrence Livermore Laboratory. An initial hypotonic KCl (75 μM) swelling of the cells (described by Gray et al.(12)) was used as a modification of the Pipes-hexylene glycol chromosome isolation buffer originally described by Wray and Stubbelfield (25). One milliter of cells (about 5×10^6 cells) suspended in isolation buffer was sheared for 15 to 30 seconds in a "Virtis 45" homogenizer run at half speed. Homogenization time was determined by monitoring the appearance of stretched chromosomes and intact nuclei. The final suspension contained about 10^8 chromosomes/ml and was stored frozen (-70° C) in isolation buffer. For flow system analysis the chromosomes were thawed, diluted with an equal volume of isolation buffer and stained with a sufficient volume of 1 mM Hoechst 33342 (a bis-benzimadazole dye available from Hoechst AG, Frankfurt, W. Germany) to give a final dye concentration of 10 μM (1).

Flow System and Optical Features

The general features of MACCS have been described previously (2,14,17). A Spectra-Physics model 171 argon ion laser equiped with ultraviolet transmitting optics was used as an excitation source. Excitation was with the combined 351 and 364 nm lines. Emission was filtered using a 418 nm cutoff filter (Schott KV 418). The split mirror previously used to direct emission to two independent photomultipliers has been replaced by a single front

surface mirror that in combination with a collecting lens yields a single emission beam which is processed through a beam splitting polarizer (9). A Soleil Babinet compensator (Halle, Berlin) set at $\lambda/2$ retardation was used to rotate the laser beam through any desired angle. When the plane of polarization of the exciting beam is made to coincide with the plane of observation (horizontal), the parallel and perpendicular emission intensities will be equal (14). The two photomultiplier outputs were balanced under this condition on signals from 1.75 μm fluorescent polystyrene microspheres (Polysciences, Warington, PA) or 70% ethanol fixed Chinese hamster spinner cells (SC-1) stained with 2 μM Hoechst 33342.

Some data were acquired using a correlated data acquisition program. This program allows one to collect multiparameter data in a correlated fashion in core memory such that data reprocessing and/or manipulation can be performed subsequent to collection. Such a procedure eliminates the requirement for accurate balancing if records at both horizontal and vertical excitation are taken. The exciting vector was restored to vertical for the actual measurement of anisotropy. Real time pulse-height analysis were performed by software-implemented algorithims.

Pulse-width Analysis

Our pulse width analysis circuit (sometimes refered to as time of flight) uses a fixed threshold method of measurement (22). The threshold level can be changed for the particular experiment

and was set at about 2% of the parallel peak emission for the experiments described below.

The theoretical basis for the pulse shape analysis corresponding to a variety of particle geometries will be presented elsewhere (T.M.J. in preparation). We restrict ourselves here to the formalism applicable to chromosome measurements.

In general, fluorescent structures with finite dimensions generate signals which are no longer Gaussian but represent the spatiotemporal convolution of the particle geometry with the laser beam. Numerous publications deal with the problem of extracting size information from pulse width measurements especially with respect to amplitude-independent estimators (9,16,22,24). We have adopted a procedure which utilizes the combined parameters of peak height (PH), integrated peak intensity (PA), and pulse width (PW) measured between the transition points of the signal with a fixed threshold discriminator. These parameters are measured simultaneously for each particle and are digitized and acquired by computer for real-time or if desired subsequent processing (2). In our instrument, the gains for the peak detector, signal integrator, and time-to-amplitude converter as well as the threshold level are independently adjustable and can be set and/or interrogated by the computer.

The laser intensity profile can be represented by the normal probability density function

$$\phi(\alpha) = \frac{1}{\sqrt{2\pi}} e^{-\alpha^2/2} \qquad (1)$$

where α is the distance d from the beam center normalized to

the standard deviation σ of the distribution ($\alpha = d/\sigma$). See figure 1. σ is related to the focused laser spot radius ω_o according to the expressions: Fig. 1

$$\sigma = \omega_o/2 \qquad (2)$$

$$\omega_o = f\lambda/\pi\omega$$

where f is the focal length of the focusing mirror (15), λ is the excitation wavelength, and ω is the radius of the laser beam at the $1/e^2$ intensity point. In our system ω = 0.8mm, λ = 0.36 μm, f = 49 mm, ω_o = 6.6 μm, and σ = 3.3 μm (we have as yet not determined σ experimentally).

The simplest possible representation of a chromosome is that of thin rod of defined length and orientation in the flow stream (figure 1). Four parameters define the system: θ, the angle of laser incidence within the stream (37° in our system (15)); δ, the angle made by the chromosome to the flow axis in the plane of incidence; β, the length L of the chromosome normalized to the beam parameter σ ($\beta = L/\sigma$) and S, the separation between the centers of the rod and the laser beam normalized to σ ($\alpha = S/\sigma$). Only α is considered to be time-dependent

$$\dot{\alpha} = v/\sigma \qquad (3)$$

where v is the flow velocity of the stream (and thus the rod).

The signal intensity corresponding to a set of values for α,β,θ,δ is given by

$$I(\alpha,\beta,\theta,\delta) = q \int_{-\beta/2}^{\beta/2} \phi(u)\, d\gamma \qquad (4)$$

$$I(\alpha, \beta, \theta, \delta) = \frac{q \cdot \sigma}{\cos(\theta+\delta)} \left[\Phi\left(\alpha \cos\theta + \frac{\beta}{2}\cos(\theta+\delta)\right) - \Phi\left(\alpha\cos\theta - \frac{\beta}{2}\cos(\theta+\delta)\right)\right]$$

where $u = \alpha\cos\theta + \gamma\cos(\theta+\delta)$; γ is a distance integration variable extending from the center of the rod to its end and normalized to σ; and q is a constant including the factors: laser intensity, fluorescence per unit length of the rod and unit excitation intensity, and overall system elect optical sensitivity. Φ is the cumulative normal distribution function

$$\Phi(x) = \int_{-\infty}^{x} \phi(\tau)\, d\tau \qquad (5)$$

Other expressions represent the peak height (PH) (achieved for $\alpha = 0$) and pulse area (PA):

$$PH = I(0, \beta, \theta, \delta) = \frac{q \cdot \sigma}{\cos(\theta+\delta)}\left[2\,\Phi\left(\frac{\beta}{2}\cos(\theta+\delta) - 1\right)\right] \qquad (6)$$

$$PA = \int_{-\alpha}^{\alpha} I \cdot d\alpha = \frac{2q\sigma}{\cos(\theta+\delta)}\left[\rho\,\Phi(\rho) + \phi(\rho) - m\,\Phi(m) - \phi(m)\right] - L \cdot a \qquad (7)$$

where

$$\rho = \alpha\cos\theta + \frac{\beta}{2}\cos(\theta+\delta) \quad \text{and} \quad m = \alpha\cos\theta - \frac{\beta}{2}\cos(\theta+\delta)$$

In our analysis we use the additional function

$$G(\alpha, \beta, \theta, \delta) = \frac{PH}{T} = \frac{I(0, \beta, \theta, \delta)}{I(\alpha, \beta, \theta, \delta)} \qquad (8)$$

which represents the ratio of the peak height (PH) to the intensity corresponding to the threshold level T.

The experimentally determined variables are PH (and thus G for a given value of T) and α which is given by 1/2 the pulse width measured at the threshold level T and normalized to σ. These parameters together with ϑ and δ uniquely determine the desired quantity β from which the rod (chromosome) length can be calculated. The required inversion of the function G (equ. 8) is implemented in the computer either in real-time (look-up tables) or by routines operating on the stored correlated data. It is important to note that the analysis does not require knowledge of the instrument factor σ and that the derived value of β is by definition amplitude-independent. The problems associated with the orientation angle δ are delt with in figure 1 and in the text.

RESULTS AND DISCUSSION

The fluorescence distribution of M3-1 Chinese hamster metaphase chromosomes stained with Hoechst 33342 (10 μM) is shown in figure 2C. The peaks correspond to particular chromosomes as shown by chromosome sorting and independent absorption measurements (12). Peaks a and b were identified as consisting of large metacentrics, peaks c and d medium metacentrics, e/f and g acrocentrics, h and i small metacentrics, with h also containing some small acrocentrics. The continuum of counts underneath the peaks depends upon the resolution of the measuring system and the amount of fluorescent debris. Fig 2

The coefficient of variation (CV) of peaks b,c,d,g,h, and i were in the range of 4.8 to 5.5% compared to a range of 2.2 to 3.3% for the analysis system used by Gray et al. (12). As a result peak e/f was not resolved into two peaks and had a higher CV (8%) as would be expected for two closely positioned but unresolved peaks. Peak a has a higher CV because the two number one homologues have a 5% difference in DNA content. Under the best of operating conditions we were sometimes able to observe splitting of peak i into two components, as shown.

For each peak shown in figure 2C, the parallel and perpendicular components of the fluorescence emission were measured for each individual chromosome. Both horizontal and vertical polarized excitation were used to measure the intensity of parallel and perpendicular fluorescence emission. For horizontal excitation the emission intensity measured by both photomultipliers

was equivalent for each chromosome class as illustated in figure 2A, top curve. Even though the output from the two optical channels had been adjusted to be the same using isotropic beads and cells, it was important to determine if all classes of anisotropic chromosomes had equivalent orthogonal emission characteristics, which they did. The plane of laser excitation was rotated to vertical for emission anisotropy measurements whereupon the perpendicular component decreased by a factor of about two and the parallel component stayed about constant. The ratio of these two intensities for each chromosome class is illustrated by the lower curve in figure 2A. From the slope of this curve and by correcting for numerical aperture effects (see below) an emission anisotropy of 0.30 was calculated.

Figure 2B illustrates the functional relationship between the true (corrected) emission anisotropy and the fluorescent intensity for individual chromosomes. The interesting dot distribution for the dimmest chromosomes graphically presents the problems of discrete digitization one can encounter. In our original measurements this problem resulted in incorrect lower values of emission anisotropy for the smaller chromosomes. To avoid such problems, the emission anisotropy for each chromosome class (peaks of figure 2C) was determined at several amplifier gain settings. In this way the emission anisotropy of each chromosome peak could be checked at several points over a suitable dynamic range. The emission anisotropy for all chromosomes was determined to be the same within experimental error. The

relatively narrow emission anisotropy distribution illustrated in figure 2D has a coefficient of variation of 5.6% and a mean value of 0.30. A projection of the dot frequency of figure 2B onto the ordinate indicates that a good deal of the broadening in figure 2D is due to the digitization problem discussed above. Indeed the emission anisotropy distributions for individual chromosomes (such as peaks a-g in figure 2C) were much tighter (CV = 3 - 4%). It is important to realize that the emission anisotropy distribution is generally not so uniform for other biological systems (9,11,18,20).

The emission anisotropy of deproteinated DNA obtained from Clostridium acidurici, Pseudomonas multivorans as well as CHO chromosomes stained with 10 μM Hoechst 33342 was measured in a static photometer and was determined to be 0.30. The uncorrected MACCS emission anisotropy value is about 10% low due to numerical aperature error. When the correction (14) was taken into account using the relationship

$$EA = (I_{\parallel} - I_{\perp})/(I_{\parallel} + 1.678I_{\perp})$$

the static and flow system determinations of EA are identical.

The highest resolution DNA chromosome distribution were always obtained using the narrowest particle stream possible. Using such a narrow stream to give as much alignment of the asymmetric chromosomes as could be obtained, the time duration of the fluorescence signal of each chromosome was measured, figure 3B. Six distinct peaks were typically resolved with the first peak (channel 70) sometimes being more completely Fig.

resolved. An electronic window was set on each peak and the corresponding fluorescence distribution measured. The gated fluorescence distributions are shown in figure 3D and 3E. Because the data in figure 3A,B,D, and E were collected simultaneously, peak positions from figures 3A were used to identify the fluorescent peaks obtained from the gated pulse width (PW) distributions, figures 3D and 3E. The results are as follows: peak 1 and I correlate, peak 2 and peak H correlate, the main peak of 3 and G, the small shoulder of 3 and F, peak 4 which is similiar in appearance to 3 correlates with E and D, peak 5 and C, and peak 6 includes peaks A and B. A repeat measurement (figure 3C) gave better resolution so that the fluorescence distribution associated with each of the first two peaks could be analyzed separately. Two DNA peaks were resolved and are shown superimposed in figure 3F. The lower intensity peak was in channel 19 with a standard deviation of 1.2 and the higher intensity peak was in channel 22 with a standard deviation of 1.5. In these two cases, PW measurements were able to resolve chromosome populations that were not resolved by DNA fluorescence.

Pulse width measurements are dependent on the relative size of the particle being analyzed, the laser beam dimensions, and the threshold setting that determines the start and stop pulse for the circuit. The question arises as to what effect the peak pulse height has on the width of the pulse at the height of the discriminator level. Two experimental results argue for the fact that the measurements are for the most part peak height

independent. The two chromosome pairs comprising peak I (figure 3A) have the same fluorescence intensity (same peak height) yet different PW values. Secondly, the number one and number two chromosomes (peak A and B) have greatly different fluorescent intensities but the same PW distribution.

A further understanding of pulse width analysis for chromosomes is found in figures 4A and 4B which compares the experimental and theoretical dependence of PW on fluorescent intensity. Theory (see materials and methods) is shown to agree well with the experimental distribution. The geometry of MACCS is such that chromosome orientations 2 and 3 (figure 1) give different theoretical curves. Four chromosome alignments were used to calculate the curves shown in figure 4A. For $\delta = \pm 45^{\circ}$ the orientation is clear from figure 1, the additional angle of $\delta = +45^{\circ}$ is the situation resulting from chromosomes tilting in a direction orthogonal to the direction of the laser beam. A chromosome in position 2 ($\delta = +45^{\circ}$) would be expected to have a minimum α (normalized pulse width) since it is almost parallel to the direction of the laser beam. A comparison of frames A and B demonstrates that for $\delta = +45^{\circ}$ the calculated value of α plateaus at the high fluorescent intensities. The data points (frame B) also appear to be defining a minimal value. No data points are found below the emerging curve in frame B. Fig. 4

For chromosome peaks a, b, and c (corresponding to a value of G or 'ratio' > 22) the calculated range of PW values increases if chromosome alignment is not perfect. One would therefore expect to see a spreading in the distribution of data points in

figure 4B for the region corresponding to the largest chromosomes if their alignment along the direction of flow is not perfect. This situation can be observed in figure 4B. The distribution of dots in figure 4B corresponding to chromosomes a,b, and c indicates that there are proportionally fewer events close to the minimal value for these larger chromosomes than is the case for smaller chromosomes. This preliminary interpretation indicates that not all of the larger chromosomes align as well as originally expected. The calculated function (figure 4A) indicates, as is logical, that the alignment of smaller chromosomes is not crucial and this is confirmed by the tight clustering of data points associated with the smaller chromosomes.

In figure 3D, gated distribution number 6 encompasses chromosome peaks a,b, and a number of counts below channel 128. The unexpected portion of the distribution (below channel 128) can be interpreted from figures 4B and 4C. A projection of the last peak of figure 4D onto figure 4B defines a horizontal slice that includes a number of counts having low fluorescence intensity. This explains why the fluorescence profile gated on the last PW peak has the distribution that it does. It is postulated that these low fluorescence counts arise from a few small chromosomes that are stretched in the isolation procedure.

CONCLUSIONS

Three independent but related measurements were made on Chinese hamster chromosomes; DNA content, emission anisotropy, and pulse width. The first and last parameters when measured simultaneously can resolve a greater number of chromosomes than either parameter by itself. The emission anisotropies for each defineable chromosome peak were also measured and determined to be the same ($E\Lambda = 0.30$). The fact that the emission anisotropy was constant for all chromosomes indicates that the molecular mobility (averaged over all dye molecules on one chromosome) is the same for all chromosome classes. The invariant emission anisotropy also indicates that there is no preferential dye binding orientation.

Pulse width measurements, while not a direct measure of chromosome arm length, give information related to the hydrodynamic length of the chromosome. This measured length will depend on fluorochrome base specificity only if base pair rich regions occur at the tip of a chromosome. The relationship that exists between a given chromosome fluorescence intensity and its PW, using a fixed threshold, was measured and found to agree with a theoretical model which also takes into account the degree of chromosome orientation. The suprisingly good pulse width resolution provides further chromosome fine structure.

LITERATURE CITED

1. Arndt-Jovin DJ, Jovin TM: Analysis and Sorting of Living Cells according to Deoxyribonucleic Acid Content. J Histochem and Cytochem 25: 585 (1977).

2. Arndt-Jovin DJ, Jovin TM: Automated Cell Sorting with Flow Systems. Ann Rev Biophys Bioeng 7: 527 (1978).

3. Arndt-Jovin DJ, Jovin TM: Cell Separation Using Fluorescence Emission Anisotropy. Membranes and Neoplasis: New Approaches and Strategies. Alan R Liss, Inc New York (1976) pp 123.

4. Arndt-Jovin DJ: unpublished results.

5. Automation of Cytogenetics, Asilomar Workshop. Edited by ML Mendelsohn, MTIS, Springfield, Va. (1976).

6. Basu S: Molecular Organization of DNA in Chromosomes. Biopolymers 16:2315 (1977).

7. Carrano AV, Gray JW, Moore DH: Purification of the Chromosomes of the Indian Muntjac by Flow Sorting. J Histochem Cytochem 24: 348 (1976).

8. Carrano AV, VanDilla MA, Gray JW: Flow Cytogenetics: A New Approach to Chromosome Analysis, Flow Cytogenetics and Sorting, Edited by MR Melamed, PF Mullaney and ML Mendelsohn, J Wiley and Sons, New York. In press.

9. Chan SS, Arndt-Jovin DJ, Jovin TM: Proximity of Lectin Receptor on Cell Surfaces Measured by Fluorescence Energy Transfer in a Flow System. J Histchem Cytochem (submitted).

10. Chromosome Identification-Technique and Application in Biology and Medicine. Edited by T Caspersson and L. Zech, Academic Press, New York (1973).

11. Epstein M, Norman A, Pinkel D, Udkoff R: Flow System Fluorescence Polarization Measurements on Fluorescein Diacetate-Stained EL4 Cells: J Histochem and Cytochem 25: 821 (1977).

12. Gray JW, Carrano AV, Steinmetz LL, VanDilla MA, Moore DH, Mayall BH, Mendelsohn ML: Chromosome Measurement and Sorting by Flow Systems. Proc Nat Acad Sci 72: 1231 (1975).

13. Human Chromosome Methodology. Edited by J Yunis, Academic Press, New York (1974).

14. Jovin TM: Fluorescence Polarization and Energy Transfer: Theory and Applications in Flow Systems, Flow Cytometry and Sorting, Edited by MR Melamed, PF Mullaney, and ML Mendelsohn, J Wiley and Sons, New York. In Press.

15. Jovin TM, Morris SJ, Striker G, Schultens HA, Digweed M, Arndt-Jovin D: Automatic Sizing and Separation of Particles by Ratios of Light Scattering Intensities. J Histochem Cytochem 24: 269 (1976).

16. Leary JF, Habbersett R, Todd P, Wood J: Pulse-Height-Independent Time of Flight Sizing of Stained and Unstained Mammalian Cells by Flow Cytophotometry. (submitted)

17. Ledley RS, Lubs HA, Ruddle FH: Introduction to Automatic Chromosome Analysis. Comput Biol Med 2: 107 (1972).

18. Lindmo T, Steen HG/ Flow Cytometric Measurement of the Polarization of Fluorrescence from Intracellular Fluorescein in Mammalian Cells. Biophys J 18: 17[illegible] (1977).

19. Mendelsohn ML, Mayall BH: Chromosome Identification by Image Analysis and Quantitative Cytochemistry, in Human Chromosome Methodology, Edited by J Yunis Academic Press, New York (1974).

20. Price GB, McCutcheon MJ, Taylor WB, Miller RG: Measurement of Cytoplasmic Fluorescence Depolarization of Single Cells in a Flow System. J Histochem Cytochem 25: 597 (1977).

21. Sharpless TK, Melamed MR: Estimation of Cell Size from Pulse Shape in Flow Cytofluorometry. J Histochem Cytochem 24: 257 (1976).

22. Steinkamp JA, Hansen KM, Crissman HA: Flow Microfluorometric and Light Scatter Measurements of Nuclear and Cytoplasmic Size in Mammalian Cells. J Histochem Cytochem 24: 292 (1976).

23. Stubbelfield E. Cram LS, Deaven L : Flow Microfluorometric Analysis of Isolated Chinese Hamster Chromosomes. Exp Cell Res 94: 464 (1975).

24. Wheeless LL, Patten SF : Slit Scan Cytofluorometry. Acta Cytol 17: 333 (1973).

25. Wray W, Stubbelfield E: A New Method for the Rapid Isolation of Chromosomes, Mitotic Apparatus, or Nuclei from Mammalian Fibroblasts at Near Neutral pH. Exp Cell Res 5: 469 (1970).

FIGURE LEGENDS

Figure 1. Chromosome and laser beam orientations used for pulse shape analysis calculations. The liquid stream is in air and contains chromosomes (long rods) with various alignments relative to the laser beam which is shown as a dotted line in air and a solid line within the stream. See text for a definition of symbols and explanation.

Figure 2. Correlated fluorescence and emission anisotropy data for 10 μM Hoechst 33342 stained Chinese hamster M3-1 metaphase chromosomes. (A) Parallel (abcissa) and perpendicular (ordinate) emission intensities using two orientations of polarized laser excitation. For horizontal excitation (90°, top line), the electric vector is orthogonal to the parallel and perpendicular planes of observation. Using isotropic beads and cells the values for $I_{\parallel}$ and $I_{\perp}$ were adjusted to be equal. The range of values is the same for both axes. Upon vertical excitation (0°, bottom line) the parallel component increased relative to the perpendicular component which is an indication of polarized emission. Each dot represents the correlated values of the intensities measured by the two photomultipliers. (B) Emission anisotropy (ordinate) for each chromosome verses the correlated fluorescent intensity (// component) of the chromosome. Full scale on the ordinate is 0.4, the theoretical maximum EA. (C) Fluorescence pulse height distribution (|| emission component) of 50,000 chromosomes where each peak corresponds to one or more metaphase chromosomes. No smoothing functions were applied and all available digitization (9 bit resolution = 512 channels) of the data was used. Peak

identification has been confirmed by flow sorting (4,12). (D) Emission anisotropy for all chromosomes. The abcissa is given in units of true EA; ie, a numerical aperature correction was made (see text). The four frames are oriented as shown to aid interpretation. The abcissa of frames A, B, and C are all equivalent so a vertical comparison can be made. Likewise the abcissa of frame D is the same as the ordinate of frame B- both axes are EA and have the same scale. The two dimensional information in frame B can be viewed as two, one dimensional plots as shown in frames C and D. Frames A and B include only 800 data points to maintain the clarity of detail for observation. With all 50,000 events displayed the pattern is the same but some of the detail shown here is lost.

Figure 3. Frequency distribution histograms for Chinese hamster M3-1 chromosomes stained with Hoechst 33342. (A) Fluorescence distribution. (B) Fluorescence pulse width distribution. (C) Fluorescence pulse width distribution run under conditions of improved resolution. (D and E) Superimposed fluorescence distributions associated with each pulse width distribution shown in frame B. (F) Superimposed fluorescence distributions associated with the right and left components of peak 1 shown in frame C. The PW windows were placed at about 15% of peak height or at the channel corresponding to the minimum value between each peak. The gated distributions in D were measured independently so the relative areas are not significant.

Figure 4. Correlated fluorescence and pulse width (PW) data for the same chromosome data set illustrated in figure 2. (A) Calculated PW function, alpha ((pulse width/2)/ σ) on the ordinate, versus the ratio (G) of chromosome peak intensity to threshold (abcissa) for four chromosome orientations. From the top; $\delta = -45^{o}$, $\delta = 0^{o}$, $\delta = +45^{o}$ but in the plane orthogonal to the laser direction, and $\delta = +45^{o}$, see figure 1. An 11 μm chromosome (chromosome number 1) would have a ratio of 47. (B) Two dimensional dot plot of correlated PW (ordinate) and fluorescent intensity (abcissa) for individual chromosomes. (C) Fluorescence pulse height distribution of 50,000 chromosomes, same as used in figure 2C. (D) Pulse width frequency distribution of chromosomes illustrated in frame C. The threshold for the PW gating was set at 2% of full scale of the channel measuring parallel emission intensity. Values for the abcissa were calculated based on a flow rate of 12.3 microns/ μsec and a value of σ for the focused laser beam of 3.3 μm. The abcissa of frames A, B, and C are scaled the same. The ordinate of frame B (pulse width) is the same as the abcissa of frame D. The data in frames B, C, and D are all from one correlated data set of 50,000 chromosomes which is also the same data set used in figure 2. An explanation of the two dimensional dot plot (B) and its relation to the data shown in (C) and (D) is included in the legend of figure 2.

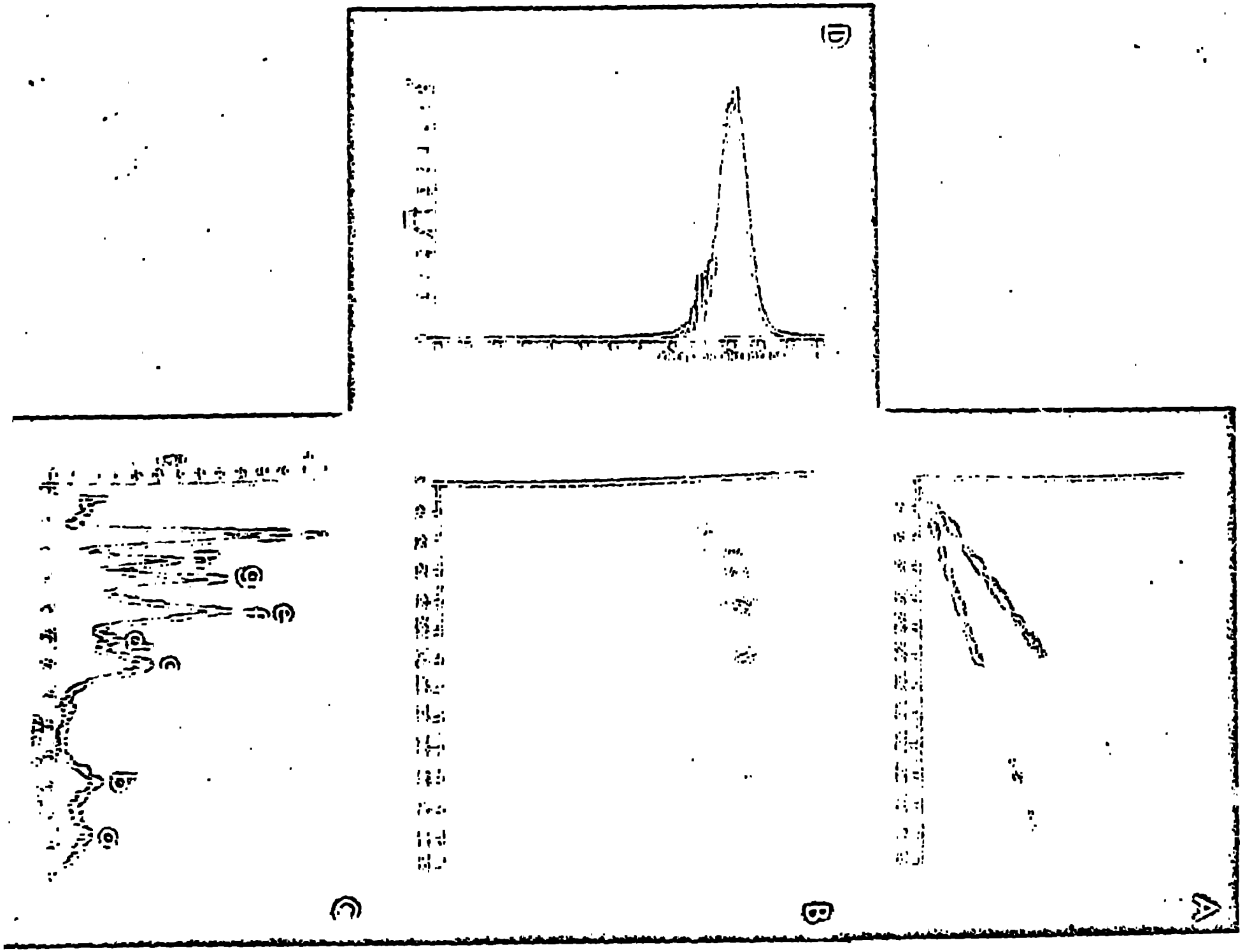
(A)
(B)
(C)
(D)

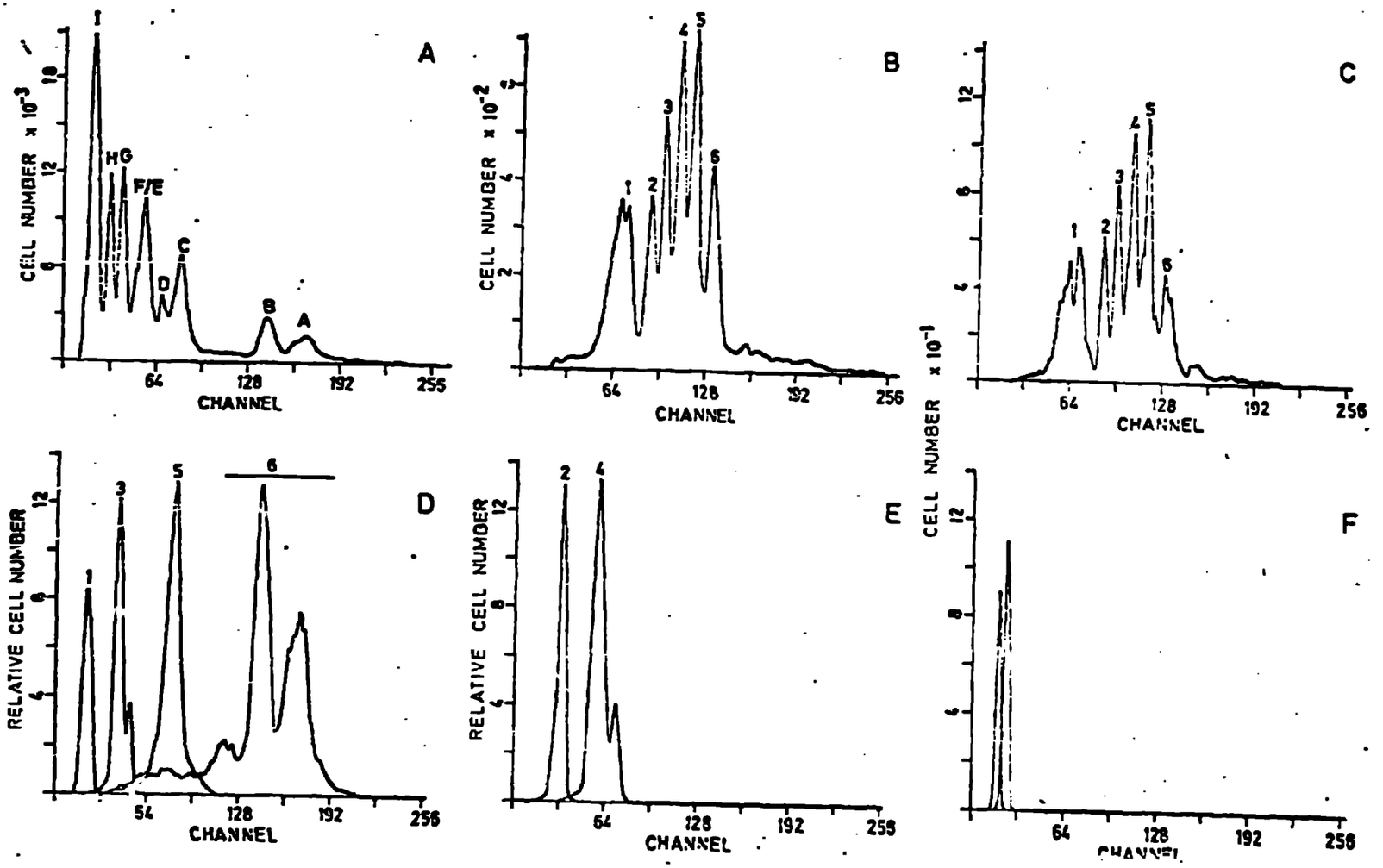
A
CELL NUMBER x 10⁻³
HG
F/E
D
C
B
A
CHANNEL
B
CELL NUMBER x 10⁻²
CHANNEL
C
CELL NUMBER x 10⁻¹
CHANNEL
D
RELATIVE CELL NUMBER
CHANNEL
E
RELATIVE CELL NUMBER
CHANNEL
F
CELL NUMBER
CHANNEL

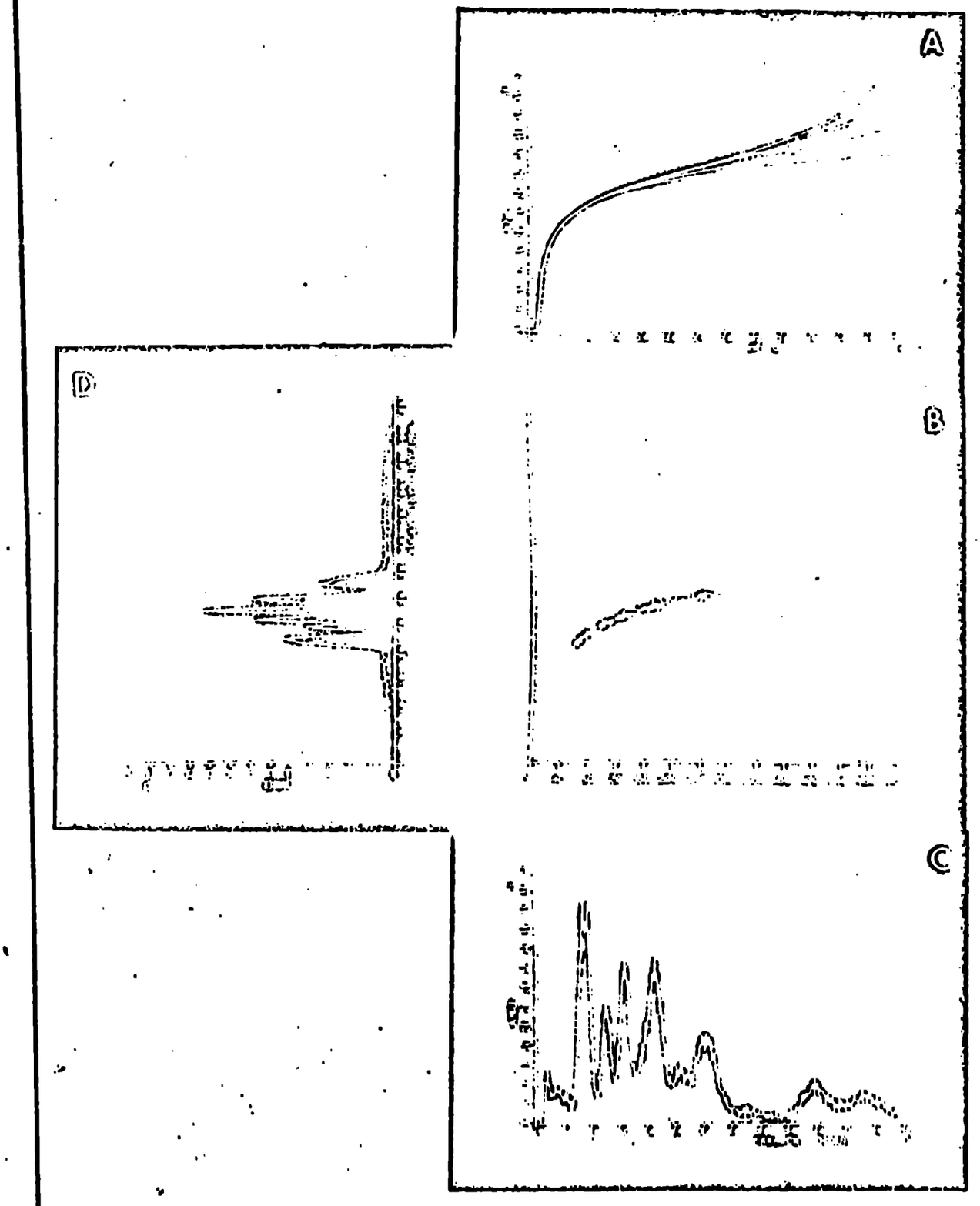
A
B
C
D

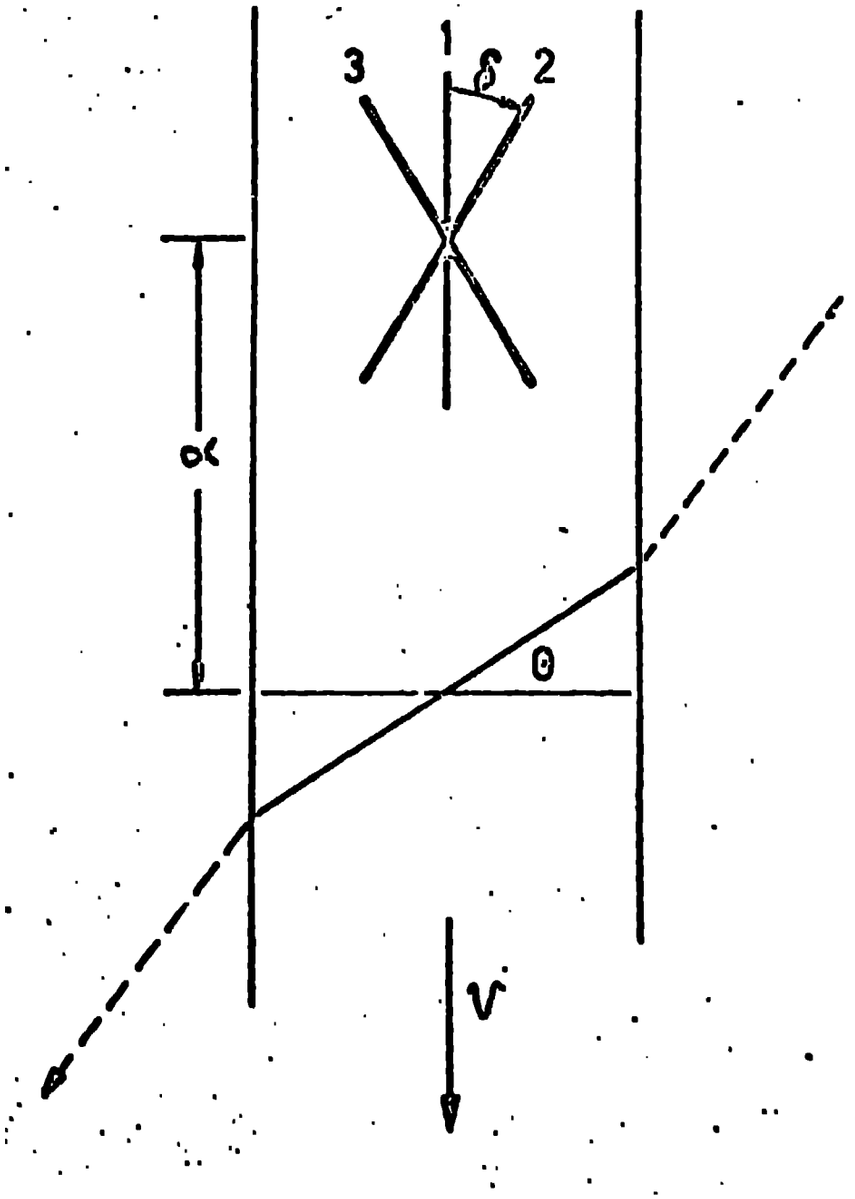
1
2
3
δ
d
θ
V